frontiers in Sustainable Food Systems

ORIGINAL RESEARCH
published: 25 March 2022
doi: 10.3389/fsufs.2022.809008

Identification and Gene Mapping of the Lesion Mimic Mutant *lm8015-3*

Chen Wang[1], *Beifang Wang*[1], *Liyong Cao*[1,2], *Yingxin Zhang*[1], *Yu Gao*[1], *Yongrun Cao*[1], *Yue Zhang*[1], *Qunen Liu*[1]* *and Xiaohui Zhang*[1,3]*

[1] *State Key Laboratory of Rice Biology, Key Laboratory for Zhejiang Super Rice Research, China National Rice Research Institute, Fuyang, China,* [2] *Northern Center of China National Rice Research Institute, China National Rice Research Institute, Fuyang, China,* [3] *Zhejiang Guodao High-Tech Seed Industry Co., Ltd., Fuyang, China*

Lesion mimic mutants (*LMM*s) exhibit spots on leaves without fungal infection pressure. The spots confer variable resistance to pathogens in different *LMM*, making them useful research materials. It is unclear how the rice immune system responds to infection with the fungal pathogen *Magnaporthe oryzae* (*M. oryzae*). Here, we identified a rice *LMM*, *lm8015-3*, which shows reduced resistance to *M. oryzae*. We used Quantitative Real-Time PCR (qRT-PCR) to observe the immune system response to *M. oryzae*–induced *lm8015-3*. *Lm8015-3*, obtained from an ethyl methane sulfonate (EMS)–induced Zhonghui8015 (ZH8015) library, showed orange-yellow spots starting in the seedling stage and accumulated more H_2O_2, resulting in severe degradation of the chloroplast. With map-based cloning, the target gene was located on chromosome 12. Once inoculated with *M. oryzae*, the expression level of pathogen-related genes of *lm8015-3* was downregulated between 48 and 72 h. In addition, more germinating spores appeared in *lm8015-3*. Therefore, we conclude that *M. oryzae* weakening the immune system of *lm8015-3* from 48 to 72 h makes *lm8015-3* more susceptible to *M. oryzae*. These results suggested that understanding how *LMM*s defend against *M. oryzae* infection will contribute to improving rice breeding.

Keywords: rice, *LMM*, ZH8015, *lm8015-3*, defense

OPEN ACCESS

Edited by:
Wei Li,
Hunan Agricultural University, China

Reviewed by:
Yuese Ning,
Institute of Plant Protection (CAAS), China
Shimin Zuo,
Yangzhou University, China
Zhiqiang Li,
Institute of Plant Protection (CAAS), China

***Correspondence:**
Qunen Liu
liuqunen202@163.com
Xiaohui Zhang
zhangxiaohui02@caas.cn

Specialty section:
This article was submitted to Agroecology and Ecosystem Services, a section of the journal Frontiers in Sustainable Food Systems

Received: *04 November 2021*
Accepted: *03 February 2022*
Published: *25 March 2022*

Citation:
Wang C, Wang B, Cao L, Zhang Yx, Gao Y, Cao Y, Zhang Y, Liu Q and Zhang X (2022) Identification and Gene Mapping of the Lesion Mimic Mutant lm8015-3. Front. Sustain. Food Syst. 6:809008. doi: 10.3389/fsufs.2022.809008

INTRODUCTION

Rice is the staple food for the majority of people in China. Improving its grain production has thus been a major research focus for many years. However, many factors reduce rice yield production, especially rice blast fungus, *M. oryzae*. *M. oryzae* is considered the most threatening pathogen to rice production, partly because it develops into spots to spread and infect more plants.

Plants have developed a strict defense response to restrict pathogens from spreading. The pathogen-associated molecular pattern (PAMP)–triggered immunity and effector-triggered immunity are two barriers in the plant defense system. The conserved PAMPs or specific effectors of microbes are essential for the plant to identify the pathogen. In the interaction between plants and pathogens (Jones and Dangl, 2006; Bent and Mackey, 2007), many molecular reactions are activated to assist the immune system, such as the production of reactive oxygen species (ROS), the secondary messengers of plant–pathogen interactions (Cheval et al., 2013; Hetmann and Kowalczyk, 2018). Hypersensitive response (HR), a symptom of programmed cell death, finally occurs within the infected area to avoid infection (Chen et al., 2012).

Lesion mimic mutants (*LMM*s) display spontaneous spots on leaves similar to the HR and usually exhibit differential resistance to pathogens without external stresses (Yoshimura et al., 1997). The first *LMM*, *sl*, was found in 1965 (Fujiwara et al., 2010), and since then, researchers have identified more rice mutants to explain the function of immune system genes in responding to pathogens. Most *LMM*s have enhanced resistance to *Pyricularia oryzae* or *Xanthomonas oryzae* pv. *oryzae* except for *spl3* and *spl6* (Kang et al., 2007; Zhang et al., 2011), which means that the immune mechanism of *LMM*s still needs to be substantiated.

RESULTS

Phenotypic Characterization of *lm8015-3*

The rice *LMM lm8015-3* was obtained from the ethyl methane sulfonate (EMS)–induced Zhonghui8015 (ZH8015) mutant library. The lower leaves first exhibited small orange-yellow spots in the seedling stage. The spots gradually spread throughout the leaves from the early tillering stage to the active tillering stage. During the harvest period, the initial spots fused into a few big spots, resulting in the death of leaves (**Figures 1A–F**). In addition, the plant height, number of productive tillers per plant, and the lengths of flag leaves of *lm8015-3* were significantly smaller than in ZH8015 (**Figures 1G–I**). These results revealed that the occurrence of leaf spots affected the growth of *lm8015-3*.

Light-Dependent Formation and Chloroplast Degradation of *lm8015-3*

Light influences spot formation of *LMM*s. Therefore, we covered part of the leaf tip of *lm8015-3* with foil to avoid exposure to natural light when the spots did not appear. One week later, we found spots on the *lm8015-3* leaves exposed to sunlight, whereas no spots formed in the leaves without exposure (**Figures 2A,B**), indicating that spot formation of *lm8015-3* was induced by natural light. Photosynthetic pigments are essential to plant growth, so we measured their contents. Compared with ZH8015, the contents of chlorophyll (Chl) and carotenoid (Car) of *lm8015-3* were significantly decreased at the tillering stage (**Figure 2C**), suggesting a deficiency in the photosynthetic pigments. By transmission electron microscopy (TEM), the chloroplast structure of leaves of *lm8015-3* was disrupted, whereas it was normal in ZH8015 (**Figures 2D,E**).

ROS Accumulation and Cell Death in *lm8015-3*

*LMM*s always correspond with abnormal antioxidation metabolism, such as the accumulation of H_2O_2 or O^{2-}. We observed H_2O_2 accumulation and apoptosis of *lm8015-3* with diaminobenzidine (DAB) and Evans Blue (EB) staining. Compared with ZH8015, more H_2O_2 and dead cells accumulated in the leaves of *lm8015-3* (**Figures 3A,B**).

Furthermore, we detected data of changes in physiological indices. The contents of soluble protein (SP) and malondialdehyde (MDA) are two key indexes that describe the extent of lipid peroxidation damage to plants. Compared with ZH8015, the SP content of *lm8015-3* decreased significantly, whereas the MDA and H_2O_2 contents increased significantly (**Figures 3C–E**). These results mean that the excessive H_2O_2 accumulation seriously damaged the lipid peroxidation in *lm8015-3* leaves. Superoxide dismutase (SOD) converts O^{2-} into H_2O_2, and catalase (CAT) and peroxidase (POD) immediately convert H_2O_2 into water. However, CAT activity decreased significantly in the leaves of *lm8015-3*, opposite to the changes in SOD and POD (**Figures 3F–H**). The abnormal enzyme activity and metabolic product content of *lm8015-3* indicated that SOD accumulation in *lm8015-3* destroyed its metabolic system.

Gene Mapping of *lm8015-3*

To identify the candidate gene related to spot formation of *lm8015-3*, we crossed 02428 and *lm8015-3* to generate F_1 individuals. All F_1 individuals showed a normal phenotype. The F_2 generation displayed a 3:1 ratio between typical plants and spotted plants, indicating that a single nuclear recessive gene controlled the spotted phenotype of *lm8015-3*. Then, we used 96 F_2 individuals with spots to generate primers over the 12 rice chromosomes (from our laboratory), and found the target gene on chromosome 12 (**Figure 4A**). We designed a series of primers to shorten the linkage interval, including C35-16, W35-6, W35-7, and W35-1 (**Figure 4B**). Finally, *lm8015-3* was localized to a 544-kb interval between C35-16 and W35-6. The sequencing results showed a single base substitution (T to A) in the first exon of *LOC_Os12g16720*, which resulted in the substitution of aspartic acid to valine (**Figure 4C**). To verify the mutation, we constructed knockout plants under the Nipponbare background. The knockout plants showed the same orange spots on leaves similar to *lm8015-3* (**Figure 4D**), as a result of the deletion or insertion of a single base in *LOC_Os12g16720*.

Reduced Resistance of *lm8015-3* to *M. oryzae*

In *LMM*s, changes in the expression levels of some defense gene always accompany the appearance of spots. We examined the expression levels of defense genes between the leaves with spots and the leaves with no spots. *PR10* and *WRKY45* were highly expressed in the leaves without spots and downregulated in leaves of *lm8015-3* with spots. The expression level of *PR1b* decreased in the leaves without spots, opposite to other genes, whereas it also displayed the same decreased tendency in general (**Figures 5A,B**). These results indicated that the appearance of spots in *lm8015-3* leads to downregulated expression of defense genes.

*LMM*s have differential resistance to pathogens. Using the spray method to induce *M. oryzae* infection, 3-week-old *lm8015-3* exhibited a more significant lesion area than ZH8015 (**Figures 5C,D**), meaning that formation of spots reduced the resistance of *lm8015-3* to *M. oryzae*. The lesions of *lm8015-3* appeared at 72 h after inoculation (HAI), earlier than in ZH8015. It seemed that 72 h is needed for *M. oryzae* to infect *lm8015-3*. After inoculation, we used the leaves of *lm8015-3* and ZH8015, ranging from 0 to 96 HAI, for qRT-PCR of defense genes (*PR10*/*PR5*/*WRKY45*). The expression levels of all three genes decreased over time (**Figures 5E–G**), suggesting that the infection of *M. oryzae* suppressed the expression of defense genes. Expression levels of defense genes in *lm8015-3* decreased before

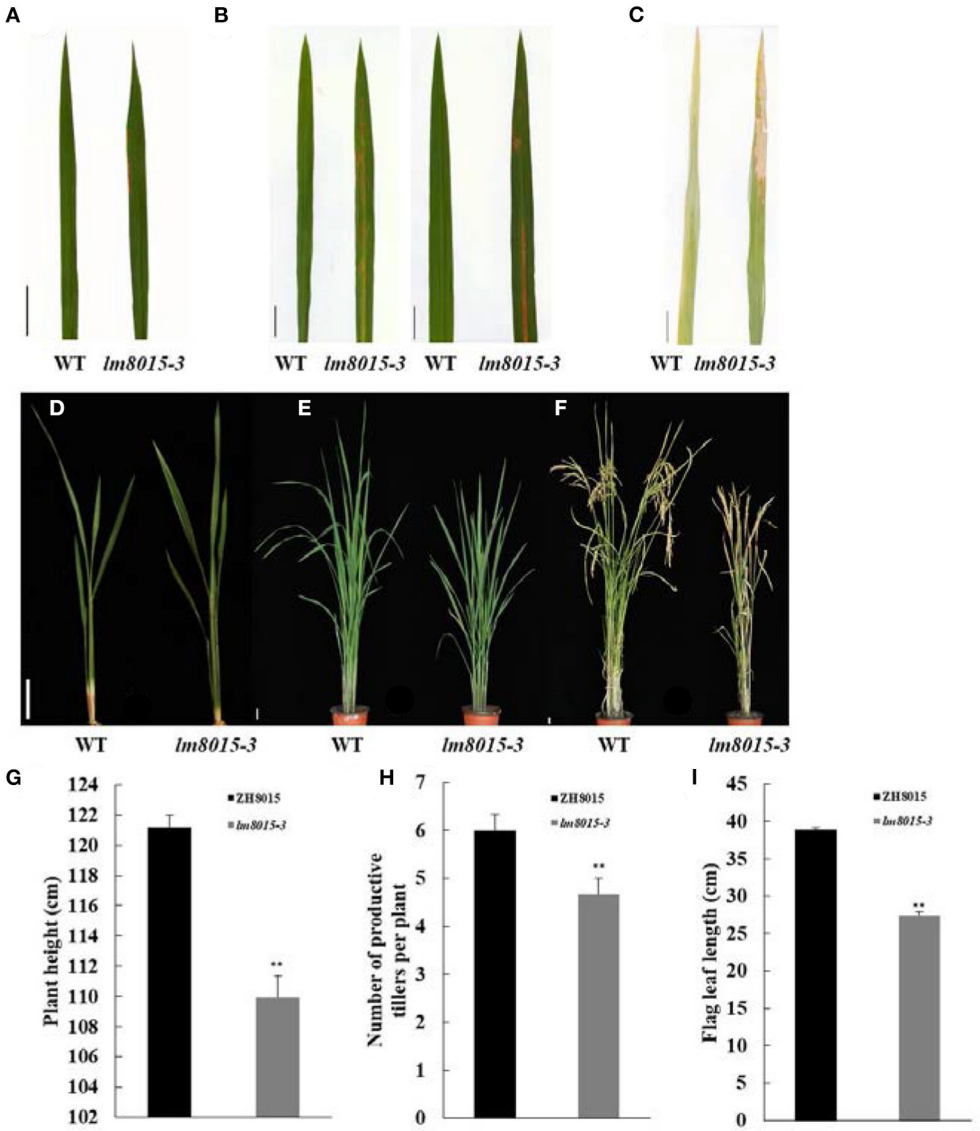

FIGURE 1 | Phenotypic characterization of the *lm8015-3* mutant. **(A–C)** Leaf phenotypes of ZH8015 and *lm8015-3* at the seedling stage, tillering stage, and mature stage. **(D–F)** Plant architecture of ZH8015 and *lm8015-3* at the seedling stage, tillering stage, and mature stage. Scale bar = 2 cm. **(G–I)** Bar graphs of plant height, number of productive tillers per plant, and flag leaf lengths of ZH8015 and *lm8015-3* measured at the mature stage. **Significant at $P < 0.01$ (*t*-test); Error bars represent SD ($n = 3$).

24 h and gradually approached ZH8015 within 48 HAI, indicating that the early defense reaction of *lm8015-3* was more sensitive than ZH8015. Expression levels of defense genes in *lm8015-3* were significantly lower than those in ZH8015 from 48 to 72 HAI, resulting in the successful infection of *lm8015-3* with *M. oryzae*. The expression level decreased from 72 to 96 HAI, which explained the delayed defense reaction of ZH8015. Therefore, *lm8015-3* was susceptible to *M. oryzae*.

As mentioned before, 72 h is required for *M. oryzae* to infect *lm8015-3*. We used leaf-sheath inoculation to determine the *M. oryzae* growth conditions in ZH8015 and *lm8015-3* at 72 h. The number of spores in *lm8015-3* was higher than in ZH8015 (**Figure 6A**) under the identified growth conditions. Most of the spores were germinating, and there were more germinating conidia in the leaves of *lm8015-3* (**Figures 6B,C**). However, the numbers of uninfected conidia and the successfully infected conidia were lower in *lm8015-3* than in ZH8015.

DISCUSSION

Previous studies have demonstrated that *sl* encodes a cytochrome P450 monooxygenase. Cytochrome P450 monooxygenase is a large family of self-oxidizing ferrous hemeprotein enzymes, named for their specific absorption peaks at 450 nm. They

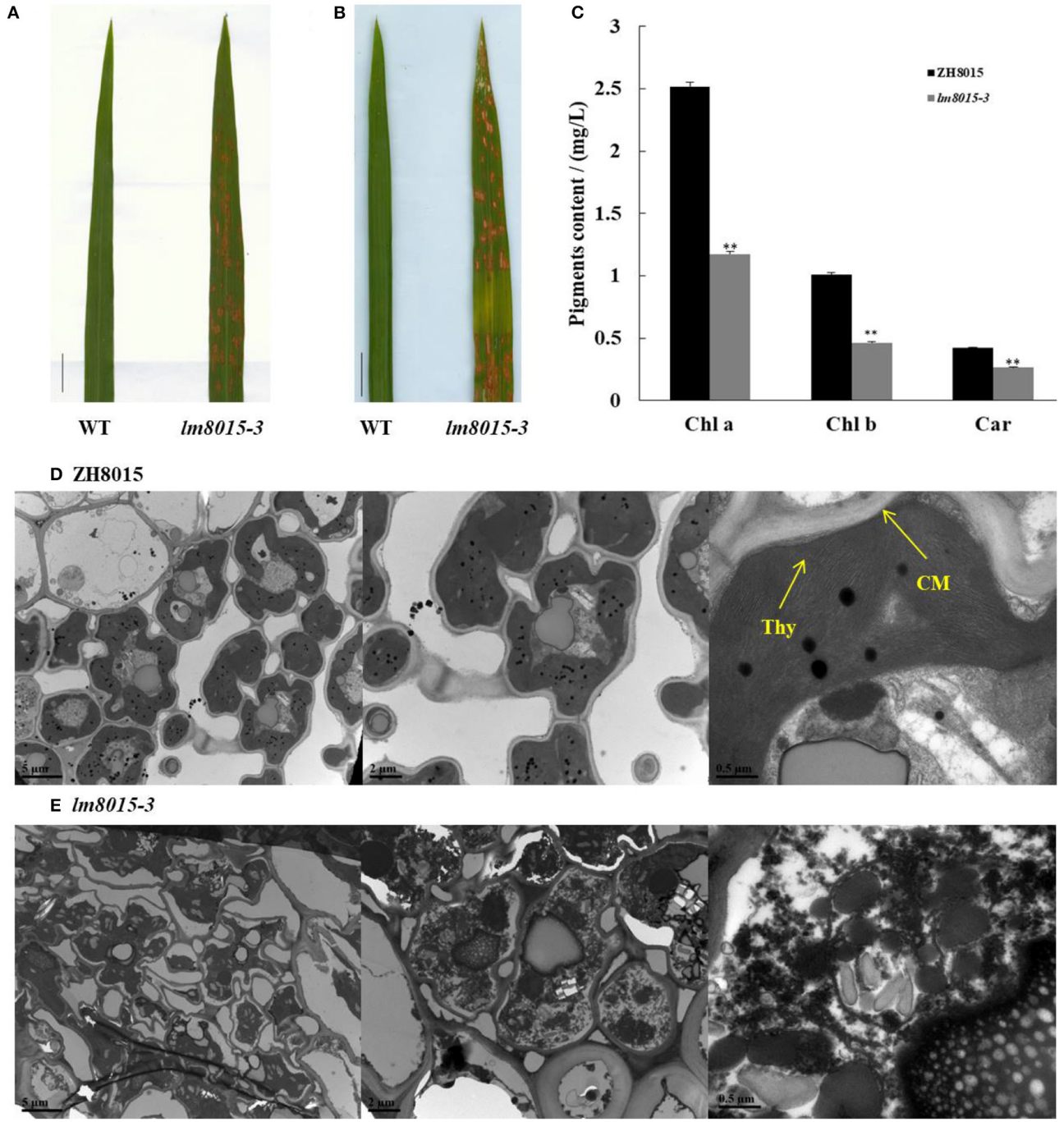

FIGURE 2 | Identification of leaves of *lm8015-3*. **(A,B)** Shading experiment of the second top leaves of ZH8015 and *lm8015-3* at the tillering stage. The leaves were exposed to light, and the leaves in **(B)** were covered with foil for 7 days; scale bar = 2 cm. **(C)** Determination of pigment contents of ZH8015 and *lm8015-3* at the tillering stage. **Significant at $P < 0.01$ (*t*-test); Error bars represent SD ($n = 3$). **(D,E)** TEM observation of the chloroplasts in ZH8015 **(D)** and *lm8015-3* **(E)** at the tillering stage. Thy, thylakoid lamellae; CM, chloroplast membrane.

are involved in the metabolism of endogenous and exogenous substances, including drugs and environmental compounds. Fujiwara et al. (2010) found that sl possesses tryptamine 5-hydroxylase activity, catalyzing tryptamine conversion to serotonin. However, the serotonin and salicylic acid (SA) pathways are antagonistic and trace back to chorismate (Maeda and Dudareva, 2012). As Lu et al. (2018) found, insect damage suppresses serotonin while inducing SA biosynthesis. Moreover,

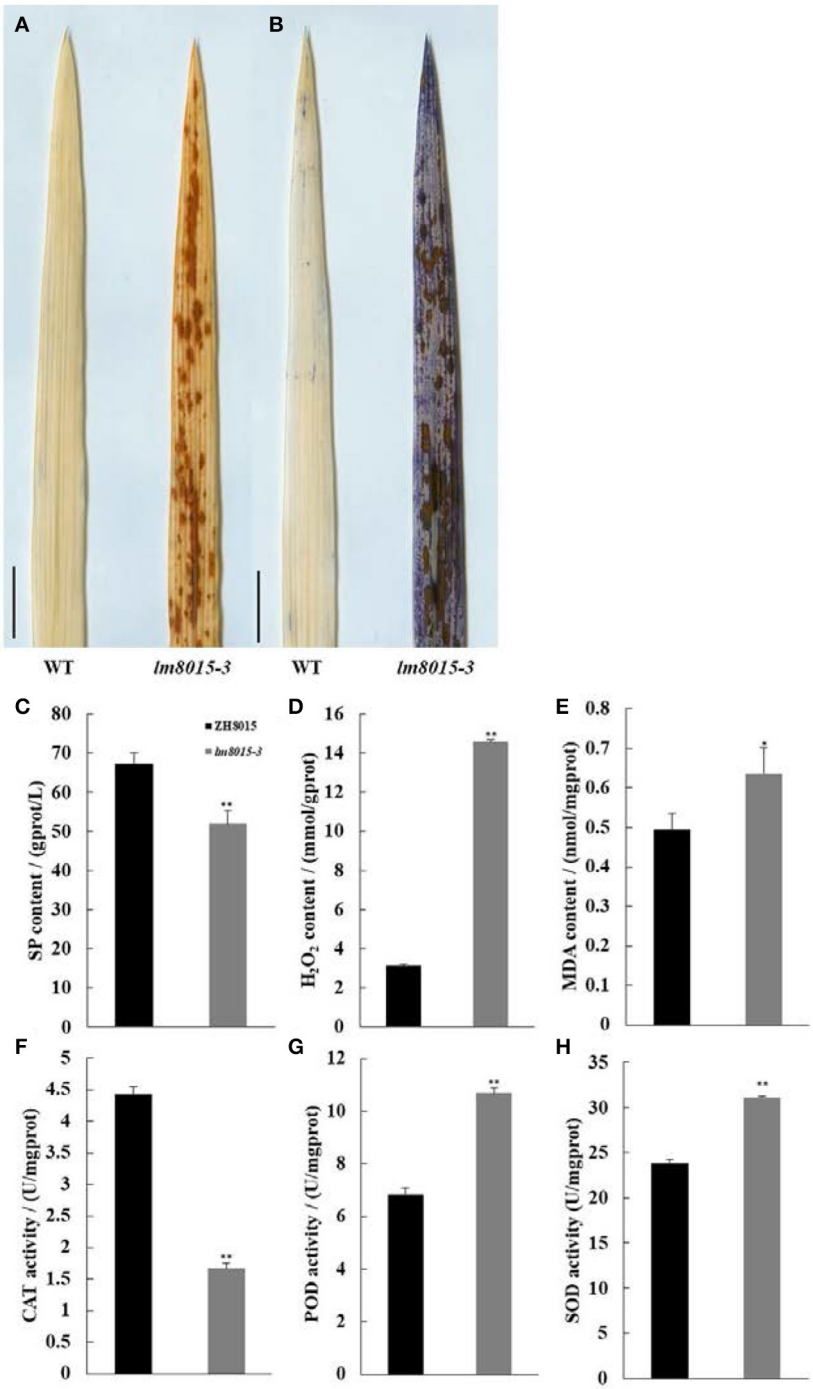

FIGURE 3 | Staining and physiological indices of ZH8015 and *lm8015-3*. **(A,B)** DAB staining and EB staining of the leaves of the wild type (ZH8015) and *lm8015-3* at the tillering stage. Scale bar = 2 cm. **(C–H)** Measurements of SP content, H_2O_2 content, MDA content, CAT activity, POD activity, and SOD activity of ZH8015 and *lm8015-3* at the tillering stage. *Significant at $P < 0.05$ (*t*-test); **Significant at $P < 0.01$ (*t*-test); Error bars represent SD ($n = 3$).

serotonin has high antioxidant activity, which could function as an oxygen radical scavenger to restrict the *M. oryzae*-induced lesion area from expanding (Hayashi et al., 2016).

Researchers previously identified more than five mutants related to *LOC_Os12g16720*; however, they exhibited differential resistance to *M. oryzae*. For example, *sl* showed reduced

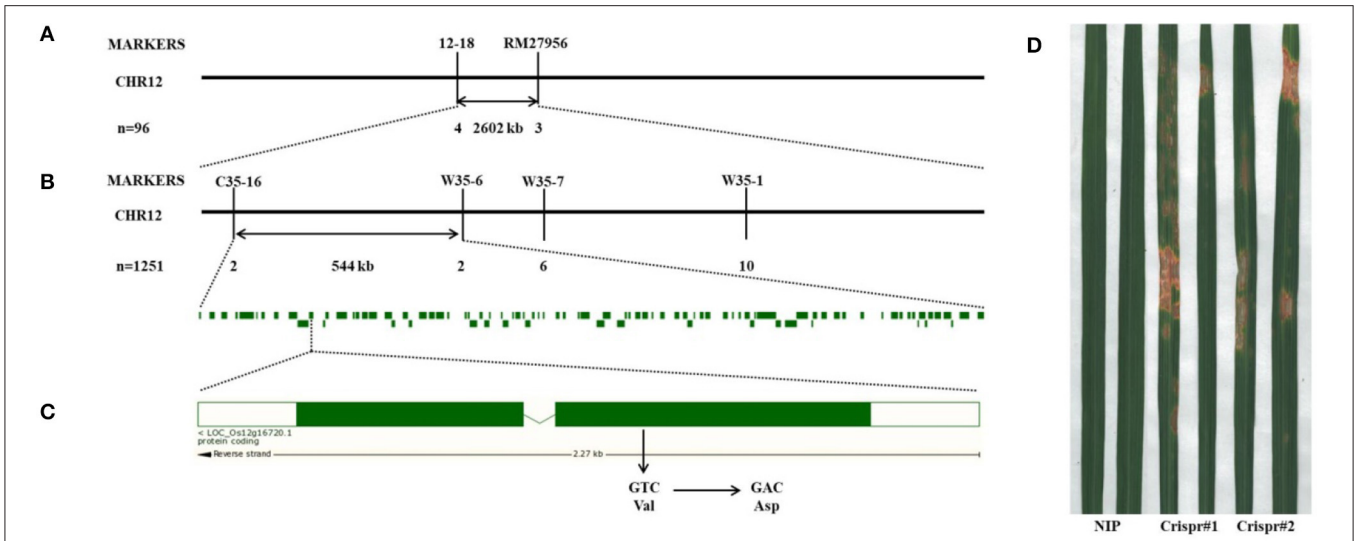

FIGURE 4 | Map-based cloning of *lm8015-3*. **(A)** *LM8015-3* was first mapped on chromosome 12 between markers 12–18 and RM27956 with 96 F_2 individuals. **(B)** *LM8015-3* was finally mapped between markers C35-16 and W35-6 with 1,251 F_2 individuals. **(C)** A single base substitution (T to A) occurred in the first exon of *LOC_Os12g16720* resulting in the mutation of Val to Asp. **(D)** The knockout plant of *LOC_Os12g16720* in Nipponbare showed the same phenotype with *lm8015-3*.

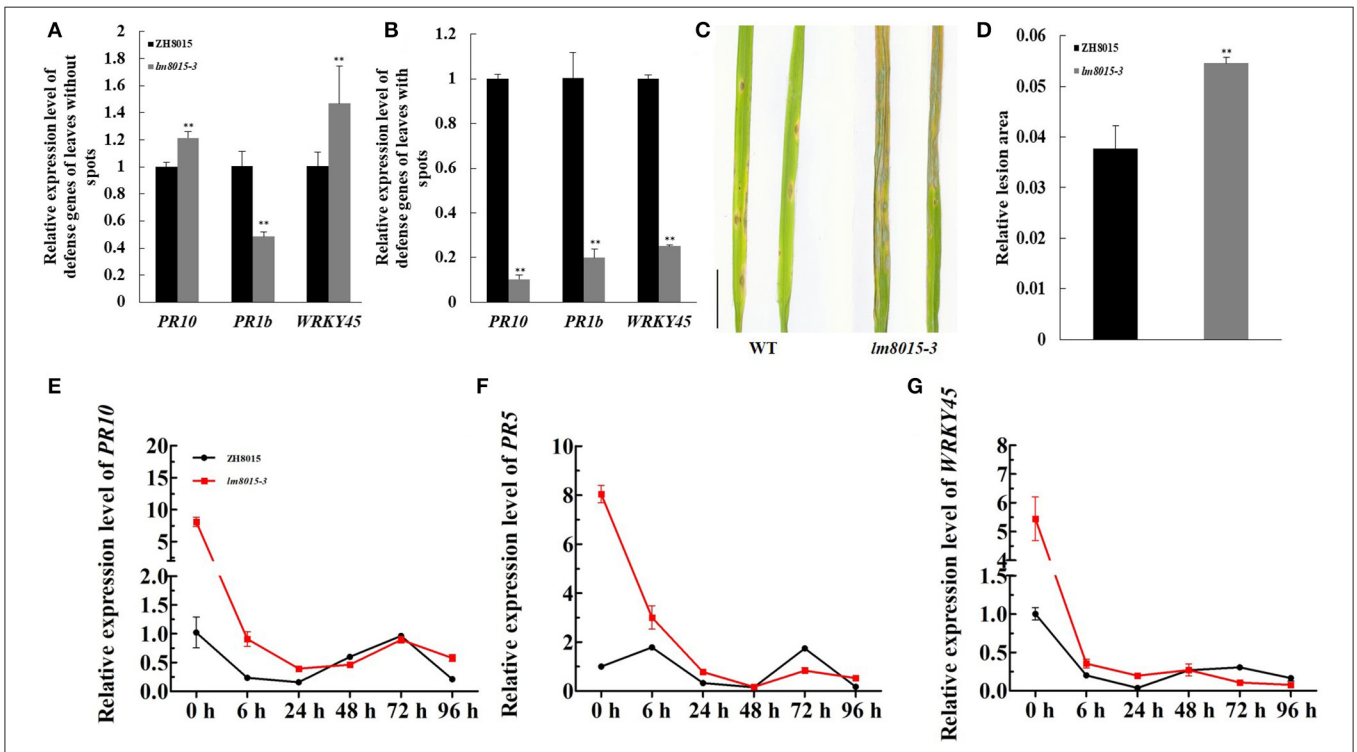

FIGURE 5 | *M. oryzae* resistance of ZH8015 and *lm8015-3*. **(A,B)** Relative expression analysis of defense genes of the leaves with and without spots. The leaves without spots were younger leaves of *lm8015-3* with no lesions at the tillering stage, whereas the leaves with spots were older leaves of *lm8015-3* with lesions at the tillering stage. **(C,D)** Spray inoculation and statistics of relative lesion area of the 3-week-old wild type (ZH8015) and *lm8015-3*. **(E–G)** Analysis of relative expression levels of *PR10*, *PR5*, and *WRKY45* of the 3-week-old ZH8015 and *lm8015-3* after inoculation. **Significant at $P < 0.01$ (*t*-test); Error bars represent SD ($n = 3$).

resistance, whereas *sl-MH* did not (Tian et al., 2020). We speculate that there are two main reasons for this phenomenon. One is the background differences between the wild type used, which might influence the genome sequence. The other more important reason is the mutation sites, which change the expression activity of *LOC_Os12g16720*. As mentioned

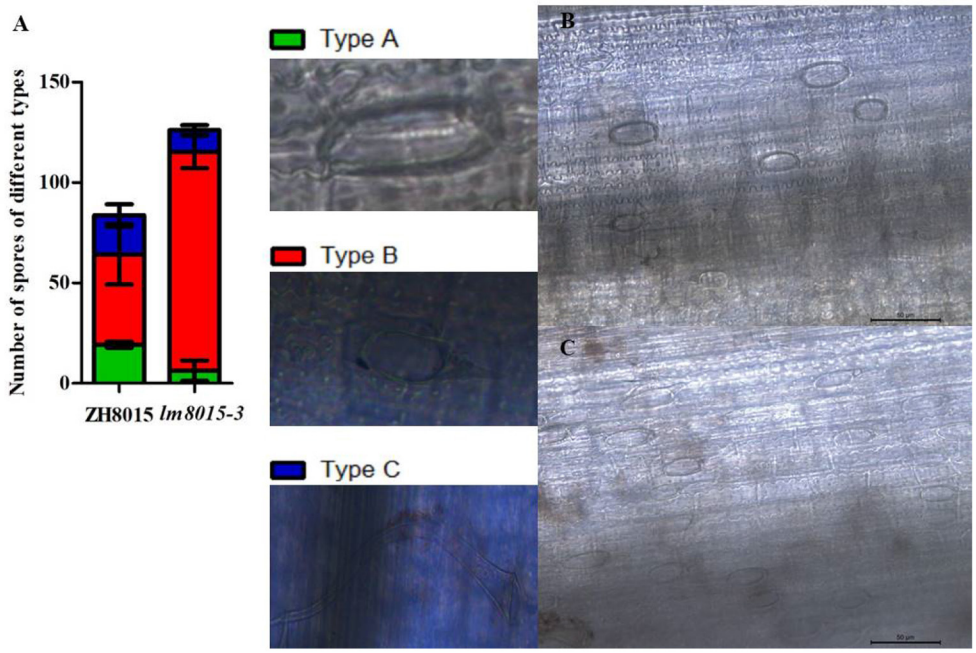

FIGURE 6 | Statistics of different spore types of ZH8015 and *lm8015-3* at 72 h after inoculation. **(A)** Graph of different types of spores of 3-week-old ZH8015 and *lm8015-3* at 72 h after inoculation; Error bars represent SD ($n = 3$). **(B,C)** The 72-h–inoculated leaf sheath of 3-week-old ZH8015 and *lm8015-3*. Type A, uninfected conidium; Type B, germinating conidium; Type C, successfully infected conidium.

before, 72 h is required for *M. oryzae* to infect *lm8015-3*. From 48 to 72 HAI, the pathogen-related genes of *lm8015-3* were downregulated compared to ZH8015, a symbol of an ineffective immune system response. *Os4CL5* and *PAL* genes are essential for lignin biosynthesis (Gui et al., 2011; Zhou et al., 2018), and *OsbHLH6* encodes a factor to regulate the signal antagonism of SA and JA (Meng et al., 2020). *Os4CL5* and *PAL7* of *lm8015-3* were downregulated, whereas *OsbHLH6* had the opposite pattern (**Supplementary Figure S1**). The biosynthesis pathways of SA, serotonin, and melatonin were identified to be involved by Lu et al. (2018), so we speculated that the SA pathway of chorismate was damaged, which means that the serotonin pathway is active. The increased level of serotonin might be the real reason for the reduced resistance of *lm8015-3*. However, the mechanism of how *M. oryzae* induces serotonin accumulation in *lm8015-3* is still unsubstantiated.

CONCLUSION

Pathogen resistance is an essential issue for rice breeding, as it can severely affect crop yield. This study identified the *LMM lm8015-3*, which exhibited reduced resistance to *M. oryzae*. The expression levels of most defense genes in *lm8015-3* were downregulated when spots appeared. The defense reaction of *lm8015-3* thus appears to be sensitive to *M. oryzae*. After the inoculation with *M. oryzae*, *lm8015-3* was easier to infect than ZH8015. Furthermore, the infected lesions on *lm8015-3* appeared 2 days earlier than ZH8015 because of the disordered immune system from 48 to 72 HAI in *lm8015-3*.

METHODS

Plant Materials and Blast Isolates

ZhongHui8015, an indica rice restorer line, was bred at the China National Rice Research Institute (CNRRI), Hangzhou, Zhejiang, China. The *LMM lm8015-3* was isolated from the ZH8015 EMS-induced library. The F_2 population derived from 02428/*lm8015-3* was used for genetic analysis and fine mapping. We measured the agronomic characteristics of *lm8015-3* and ZH8015 at the harvest period with three biological replicates, including plant height, numbers of productive tillers per plant, and flag leaf length. All materials were grown in the FuYang experimental base of CNRRI. The *M. oryzae* strain 14-1 was virulent to ZH8015.

Shading Experiment

At the tillering stage, the second top leaves without lesions of *lm8015-3* and ZH8015 were shaded with 4-cm-wide foil for 7 days, and then, the foil was removed and the leaves were photographed.

Measurements of Photosynthetic Pigment Contents

As described before (Arnon, 1949; Schippers et al., 2015), the second top leaves of plants with lesions at the tillering stage were used to measure the contents of photosynthetic pigments. Each

experiment was performed with three biological replicates. We used the means of three replicates for the *t*-test.

Chloroplast Structure Observation

For the TEM observation of chloroplast structure, the leaves of *lm8015-3* and ZH8015 at the tillering stage were first soaked in 2.5% glutaraldehyde for 24 h. Then, we sent samples to Zhejiang University for subsequent treatments.

Histochemical Analysis

The leaves of *lm8015-3* and ZH8015 at the tillering stage were stained with DAB and EB to observe the H_2O_2 accumulation and cell death as described previously (Thordal-Christensen et al., 1997; Li et al., 2004).

Physiological Indexes

Following the instructions of kits from the Nanjing JianCheng Bioengineering Institute, we ground the leaves of *lm8015-3* and ZH8015 at the tillering stage into homogenates to test the content of SP, MDA, H_2O_2, and the activities of SOD, POD, and CAT. Three replications were used for each group. The means of three replicates were used for the *t*-test.

Gene Mapping

As described previously (Rogers and Bendich, 1985), DNA of the mapping group was extracted using Cetrimonium Bromide (CTAB). Genome sequences of rice cultivars were downloaded from http://ensembl.gramene.org/ and http://rice.genomics.org.cn/, and differences between the genome sequences of the japonica cultivar Nipponbare and the indica cultivar 9311 were used to design primers for map-based cloning of *lm8015-3*. With the databases GRAMENE (http://ensembl.gramene.org/) and MSU (http://rice.uga.edu/), we designed primers for genes and analyzed the sequence differences. The PCR followed the instructions of Vazyme (P222-01). To construct knockout plants of *LOC_Os12g16720*, we used pCAMBIA1305.1 vector to delete or insert a single base in the exon. The primers for gene mapping and confirmation are listed in **Supplementary Table S1**.

qRT-PCR Analysis

Following kit instructions for Invitrogen TRIzol (Thermo Fisher), all RNA samples were extracted. To determine whether lesion occurrence changed the expression levels of defense genes, we extracted RNA of the leaves with or without lesions of *lm8015-3* at the tillering stage. In the qRT-PCR of defense genes after inoculation, the 3-week-old leaves RNA of *lm8015-3* and ZH8015 at 0, 6, 24, 48, 72, and 96 HAI were extracted. With SYBR qPCR Master Mix of Vazyme (Q511-02), three replicates were used for each group. The means of three replicates were used for the *t*-test. The primers for qRT-PCR are listed in **Supplementary Table S1**.

Blast Inoculation

M. oryzae strain 14-1, which was virulent to ZH8015, was cultured on oatmeal agar medium for 2 weeks under light for sporulation. We sprayed the 3-week-old leaves of *lm8015-3* and ZH8015 with a conidial suspension of 2×10^5 spores/ml in the growth chamber. We measured the relative infected-lesion area of *lm8015-3* and ZH8015 by relative pixels with Photoshop. The detached sheath of 3-week-old *lm8015-3* and ZH8015 leaves was injected with a conidial suspension of 1×10^6 spores/ml in the growth chamber by leaf sheath inoculation (Li et al., 2011). After 72 h, the sample was placed under a microscope and observed with a 40× objective. The number of each spore type, observed in 10 random fields of view, was used to calculate one biological replicate. Three biological replicates were used for each group. The means of three replications were used for the *t*-test.

DATA AVAILABILITY STATEMENT

The datasets presented in this study can be found in online repositories. The names of the repository/repositories and accession number(s) can be found in the article/**Supplementary Material**.

AUTHOR CONTRIBUTIONS

XZ and QL contributed to conception and design of the study. CW finished all the experiments and wrote the manuscript. BW, LC, YXZ, YG, YC, and YZ contributed to the completion of the study. All authors contributed to manuscript revision, read, and approved the submitted version.

FUNDING

This study was supported by grants from the National Natural Science Foundation of China (31871236 and 31801726) and the Agricultural Science and Technology Innovation Program of the Chinese Academy of the Agricultural Sciences (CAAS-ASTIP-2013-CNRRI).

SUPPLEMENTARY MATERIAL

The Supplementary Material for this article can be found online at: https://www.frontiersin.org/articles/10.3389/fsufs.2022.809008/full#supplementary-material

REFERENCES

Arnon, D. I. (1949). Copper enzymes in isolated chloroplasts. Polyphenoloxidase in beta vulgaris. *Plant Physiol.* 24, 1–15. doi: 10.1104/pp.24.1.1

Bent, A. F., and Mackey, D. (2007). Elicitors, effectors, and R genes: the new paradigm and a lifetime supply of questions. *Annu. Rev. Phytopathol.* 45, 399–436. doi: 10.1146/annurev.phyto.45.062806.094427

Chen, M., Zeng, H., Qiu, D., Guo, L., Yang, X., Shi, H., Zhou, T., and Zhao, J. (2012). Purification and characterization of a novel hypersensitive response-inducing elicitor from *Magnaporthe oryzae* that triggers defense response in rice. *PLoS ONE.* 7, e37654. doi: 10.1371/journal.pone.0037654

Cheval, C., Aldon, D., Galaud, J. P., and Ranty, B. (2013). Calcium/calmodulin-mediated regulation of plant immunity. *Biochim. Biophys. Acta.* 1833, 1766–1771. doi: 10.1016/j.bbamcr.2013.01.031

Fujiwara, T., Maisonneuve, S., Isshiki, M., Mizutani, M., Chen, L., Wong, H. L., et al. (2010). Sekiguchi lesion gene encodes a cytochrome P450 monooxygenase that catalyzes conversion of tryptamine to serotonin in rice. *J. Biol. Chem*. 285, 11308–11313. doi: 10.1074/jbc.M109.091371

Gui, J., Shen, J., and Li, L. (2011). Functional characterization of evolutionarily divergent 4-coumarate:coenzyme a ligases in rice. *Plant Physiol*. 157, 574–586. doi: 10.1104/pp.111.178301

Hayashi, K., Fujita, Y., Ashizawa, T., Suzuki, F., Nagamura, Y., and Hayano-Saito, Y. (2016). Serotonin attenuates biotic stress and leads to lesion browning caused by a hypersensitive response to *Magnaporthe oryzae* penetration in rice. *Plant J*. 85, 46–56. doi: 10.1111/tpj.13083

Hetmann, A., and Kowalczyk, S. (2018). Membrane receptors recognizing MAMP/PAMP and DAMP molecules that activate first line of defence in plant immune system. *Postepy Biochem*. 64, 29–45. doi: 10.18388/pb.2018_103

Jones, J. D., and Dangl, J. L. (2006). The plant immune system. *Nature*. 444, 323–329. doi: 10.1038/nature05286

Kang, S. G., Matin, M. N., Bae, H., and Natarajan, S. (2007). Proteome analysis and characterization of phenotypes of lesion mimic mutant spotted leaf 6 in rice. *Proteomics*. 7, 2447–2458. doi: 10.1002/pmic.200600961

Li, R., Lqn, S. Y., and Xu, Z. X. (2004). Studies on the programmed cell death in rice during starchy endosperm development. *Agric. Sci. China*. 3, 663–670.

Li, W., Zhong, S., Li, G., Li, Q., Mao, B., Deng, Y., et al. (2011). Rice RING protein OsBBI1 with E3 ligase activity confers broad-spectrum resistance against *Magnaporthe oryzae* by modifying the cell wall defence. *Cell Res*. 21, 835–848. doi: 10.1038/cr.2011.4

Lu, H. P., Luo, T., Fu, H. W., Wang, L., Tan, Y. Y., Huang, J. Z., et al. (2018). Resistance of rice to insect pests mediated by suppression of serotonin biosynthesis. *Nat. Plants*. 4, 338–344. doi: 10.1038/s41477-018-0152-7

Maeda, H., and Dudareva, N. (2012). The shikimate pathway and aromatic amino acid biosynthesis in plants. *Annu. Rev. Plant Biol*. 63, 73–105. doi: 10.1146/annurev-arplant-042811-105439

Meng, F., Yang, C., Cao, J., Chen, H., Pang, J., Zhao, Q., et al. (2020). A bHLH transcription activator regulates defense signaling by nucleo-cytosolic trafficking in rice. *J. Integr. Plant Biol*. 62, 1552–1573. doi: 10.1111/jipb.12922

Rogers, S. O., and Bendich, A. J. (1985). Extraction of DNA from milligram amounts of fresh, herbarium and mummified plant tissues. *Plant Mol. Biol*. 5, 69–76. doi: 10.1007/BF00020088

Schippers, J. H., Schmidt, R., Wagstaff, C., and Jing, H. C. (2015). Living to die and dying to live: the survival strategy behind leaf senescence. *Plant Physiol*. 169, 914–930. doi: 10.1104/pp.15.00498

Thordal-Christensen, H., Zhang, Z. G., Wei, Y. D., and Collinge, D. B. (1997). Subcellular localization of H_2O_2 in plants. H_2O_2 accumulation in papillae and hypersensitive response during the barley-powdery mildew interaction. *Plant J*. 11, 1187–1194. doi: 10.1046/j.1365-313X.1997.11061187.x

Tian, D., Yang, F., Niu, Y., Lin, Y., Chen, Z., Li, G., et al. (2020). Loss function of SL (sekiguchi lesion) in the rice cultivar Minghui 86 leads to enhanced resistance to (hemi) biotrophic pathogens. *BMC Plant Biol*. 20, 507. doi: 10.1186/s12870-020-02724-6

Yoshimura, A., Ideta, O., and Iwata, N. (1997). Linkage map of phenotype and RFLP markers in rice. *Plant Mol. Biol*. 35, 49–60. doi: 10.1023/A:1005764026871

Zhang, H., Liu, K., Zhang, X., Tang, W., Wang, J., Guo, M., et al. (2011). Two phosphodiesterase genes, PDEL and PDEH, regulate development and pathogenicity by modulating intracellular cyclic AMP levels in *Magnaporthe oryzae*. *PLos ONE*. 6, e17241. doi: 10.1371/journal.pone.0017241

Zhou, X., Liao, H., Chern, M., Yin, J., Chen, Y., Wang, J., et al. (2018). Loss of function of a rice TPR-domain RNA-binding protein confers broad-spectrum disease resistance. *Proc. Natl. Acad. Sci. USA*. 115, 3174–3179. doi: 10.1073/pnas.1705927115

Conflict of Interest: XZ was employed by the Zhejiang Guodao High-Tech Seed Industry Co., Ltd.

The remaining authors declare that the research was conducted in the absence of any commercial or financial relationships that could be construed as a potential conflict of interest.

Publisher's Note: All claims expressed in this article are solely those of the authors and do not necessarily represent those of their affiliated organizations, or those of the publisher, the editors and the reviewers. Any product that may be evaluated in this article, or claim that may be made by its manufacturer, is not guaranteed or endorsed by the publisher.